Technical Principles and Protocols of PET/MR Imaging

3

A. Kalemis

Contents

Introduction

PET and MRI are two well-established medical imaging modalities that are used frequently as diagnostic tools in a wide range of clinical indications providing complementary information [1]. MRI can provide anatomical information with very high spatial resolution, and functional measurements at organ and tissue level with high diagnostic sensitivity. On the other hand, PET images functional processes at cellular and sub-cellular level with very high diagnostic specificity and high tracer detection sensitivity (10^{-11}–10^{-12} mol/l) [2] but with a spatial resolution inferior to MRI. This complementary matching of capabilities renders both PET(/CT) and MRI necessary in several disease pathways, particularly in oncology and neurology. A significant workflow limitation, when both modalities are needed, is the physical and organisational separation of the two systems [3]. Patients who need both PET and MR imaging are often referred for such scans independently and, often, they are scanned with a significant time difference. This renders the fusion of information from both examinations difficult or even impossible due to disease status changes or several other technical and organisational factors [4]. Hence, when MRI is the preferred imaging modality versus CT, PET/MR should be more clinically useful than PET/CT and a combined single examination could provide significant benefits to both the patient and the hospital.

Today, there are two different designs for combined PET/MR systems; positioning PET inside the MRI magnet or in tandem, similar to PET/CT [5]. Both philosophies attempt to balance clinical utility, user flexibility in developing clinically-relevant PET/MR-dedicated imaging protocols, potential sacrifices in relation to stand-alone state-of-the-art PET and MRI imaging capabilities and cost. Irrespectively, of the design and technical differences with the stand-alone systems, PET/MR, as a novel imaging option, requires significant innovation at various levels in order to surpass current concerns and scepticism. The latter are of clinical, organisational and technological nature. Questions about how it compares with PET/CT, under which clinical

A. Kalemis
PET/MR, Philips Healthcare,
Guildford Business Park, Guildford, Surrey GU2 8XH, UK
e-mail: antonis.kalemis@philips.com

O. Ratib et al. (eds.), *Atlas of PET/MR Imaging in Oncology*,
DOI 10.1007/978-3-642-31292-2_3,

scenarios either of them should be used, patient throughput, ease of workflow, building and running costs, ownership of device and staff (between different departments), reliability of new the technology and image quality in comparison to stand-alone systems are common discussion points.

Operational Requirements

It is common in healthcare for radical new technologies to require a second innovation wave, in the area of its structure and organisation, in order to optimise their contribution in disease management and patient pathway [6]. An organisation wishing to adopt PET/MR, in particular, has to overcome its complicated logistics, often the single-modality trained technical personnel, the staffing requirement from two different departments and the excessive scanning time required to acquire both PET and MR scans, which raises significantly the cost of each scan. At this level, institutions are requested to innovate in order to successfully adopt this novel technology.

At infrastructure level, some degree of cross-departmental collaboration and in some cases even restructuring is necessary to bring the Nuclear Medicine (NM) and Radiology staff much closer. Dual-training of the technical personnel is essential in order to operate the scanner while another long-term consideration is the need to cross-train Radiologists and Nuclear Medicine physicians from both modalities [7]. However, such needs are not straightforward due several factors, amongst others the existing territorial and protective practices in many healthcare facilities and the variations in the legal frameworks for imaging technologists [8]. In many hospitals Radiology and NM departments are far from each other creating further complications in staff allocation and/or logistics of the new scanners. Therefore, a successful model needs to be devised for the placement of the scanner considering its heavy needs for MR, PET and Radiochemistry expert support while residing within a controlled area for radiation and high magnetic fields.

Innovation is also needed in defining new imaging procedures that consider the extra time and find workarounds. Depending on the patient population of the institution, the staff and the other medical imaging scanners, a different departmental (or cross-departmental) workflow may be necessary to optimise the use of all systems and personnel. A sound business case that demonstrates the added value of PET/MR in comparison to PET/CT, MRI or concurrent referrals to both modalities (i.e. the current clinical practice) [9] is also necessary to demonstrate a favourable cost/benefits balance, to these other alternatives [10, 11]. Competition is not just in the area of clinical use; procurement for PET/MR will also compete against PET/CT and MRI due to limitations in funding, space within hospitals, personnel and attracting research grants. Therefore, in order to succeed, the new modality must demonstrate better qualities than its rivals. From the system perspective, these qualities translate into superior diagnostic accuracy, a feasible workflow, adequate patient throughput and comfort, as well as imaging protocol flexibility that facilitates optimisation.

PET/MR Applications

It is still uncertain whether PET/MR will become a routine clinical imaging modality. The lack of solid evidence for its benefits on specific clinical indications, compared with PET/CT and MRI entails, at the time this book was written, the absence of any reimbursement framework for joint PET/MR scans. Therefore, the first and foremost need is the identification of those clinical indications that PET/MR excels over 'conventional' imaging in diagnostic accuracy, workflow or reduction of overall costs to an extend that referring physicians consider sending their patients for scans and healthcare regulatory authorities provide the appropriate reimbursement for such procedures. However, the experience with PET/CT shows that even when validated clinical applications are found, they will require further time to gain patient referrals and receive reimbursement [9].

Several editorials and review papers have been published, the last few years, discussing potential applications for PET/MR, based on current experience from PET(/CT) and MRI [1, 3, 4, 12–16]; while many groups use the stand-alone modalities in investigational studies and assess the benefits of combining multi-modal information in staging, therapy monitoring and disease follow-up. Recently, the first studies on clinical use have started to appear in scientific literature.

One of the potential applications that PET/MR could have an impact is on brain imaging. PET has several attractive features such as high sensitivity and specificity in detecting biochemical and molecular tracers, while its inherent poor spatial resolution can be improved by recent advances in image reconstruction that incorporate resolution recovery approaches [17, 18]. Even more importantly, however, fusing quantitative PET images with high-resolution MR anatomical images can enhance the information extracted from both modalities, while at the same time advanced MR techniques, such as diffusion weighted imaging (DWI), perfusion with MR contrast agents, functional activation (fMRI), MR spectroscopy (MRS) or Diffusion Tensor Imaging (DTI), may yield complementary to PET information [12]. In Table 3.1, a thorough list of the biological properties that can be assessed by MRI and PET is presented.

So far, very limited work has been published in brain imaging using integrated PET/MR systems. In Neuro-Oncology, two groups performed feasibility studies in

Table 3.1 Biological properties that can be assessed by PET and MRI

MRI	PET
Morphology	Flow ($H_2{}^{15}O$)
Water motion in tissue (DWI)	Metabolism (^{18}F-FDG)
Vascular anatomy (MRA)	Blood volume ($C^{15}O$)
Perfusion (PWI, DCE-MRI)	Oxygen consumption (^{15}O)
Tissue metabolites (MRS for ^{1}H, ^{13}C, ^{23}Na, ^{31}P)	Vascular permeability (labelled AA)
Functional activation (fMRI)	Nucleic acid synthesis (^{18}F-FLT)
Cerebral fibre tracts (DTI)	Transmitters (e.g. DOPA)
Oxygen consumption (^{17}O)	Receptors (e.g. Raclopride)
Migration of cells (Fe labelling)	Enzymatic activity (e.g. MP4A)
	Angiogenesis (e.g. ^{18}F-RGB)
	Tracer & drugs (labelled compounds) distribution & kinetics
	Enzymatic activity in transfected cells

Adapted from Heiss [12]

patients with intracranial masses using different PET tracers (^{18}F-FDG, ^{11}C-methionine, ^{68}Ga-DOTATOC) combined with anatomical-MR, DTI, arterial spin labelling (ASL) and/or proton-spectroscopy [19, 20]. A different study also found that DTI-MR/PET provided important information for the treatment planning of brain tumours in four patients [21]. Neuner et al. have also demonstrated the use of ^{18}F-FET and ^{11}C-Methionine in combination with anatomical MRI, DTI, MRS and fMRI in PET/MR [22]. Finally, several groups have also shown the benefits of combined PET and MR information using stand-alone systems. Some of such applications include glioma staging [15], therapy planning [23, 24] and differential diagnosis from inflammatory demyelination [25]; therapy response of glioblastomas [26] and meningiomas [27]; as well as in image-guided neurosurgery for brain tumours [28, 29]. Apart from neuro-oncology, PET/MR may be useful in the assessment of damage inflicted by stroke [30], or as shown recently in neurodegenerative diseases [31–34], as well as epilepsy [35–37]. Furthermore, there are literature reports of combined PET and MRI use for various research studies, amongst others, in schizophrenia [38, 39], addictions [40], autism [41], aphasia [42] and multiple sclerosis [43].

Today, all the commercial PET/MR tomographs are designed with whole-body imaging capabilities, as this is necessary in order to perform oncological and cardiac scans. Advanced cardiovascular imaging is expected to be another opportunity for PET/MR given the excellent attributes of cardiac MRI and PET's absolute quantification [44]. Publications that demonstrate the successful combination of PET and MR imaging already exist in cardiomyopathy [45], evaluation of myocardial infarction [46] and its response to different therapy schemes [47, 48] and evaluation of carotid artery stenosis [49]. Therefore, although clinical evidence using integrated systems is still under way, PET/MR is expected to be a very useful modality for cardiovascular imaging [44].

Oncology is the main application of PET with highest volumes of scans globally and one of the areas with the biggest procedures growth for MRI. Moreover, the combination of these two modalities exhibit complementary advantages such as enhanced accuracy in the staging of primarily disease as well as in the assessment of local lymph node involvement and distant metastases [50]. Pilot studies with integrated systems have already shown the feasibility [51] of oncological PET/MR and potential clinical benefits in head and neck cancer [52], and lung cancer [53]; while its use was also showcased in single case studies for indications such as paediatric oncology [16], prostate [54, 55] and therapy follow up for malignancies of the liver [56]. Extensive discussions of the expected benefits of PET/MR in oncology can be found in literature [50, 57, 58].

Clinical Protocols and Workflow Considerations

An important concern for PET/MR scans is time. Both PET and MRI require long acquisition times for a comprehensive examination. Extended scan times have an impact on patient comfort (and increase of drop-out rates) and throughput, increasing the cost per scan. Therefore, some consideration on how to reduce acquisition time without losing important information is necessary for the various applications and the two system designs. Imaging acquisitions can be classified in two groups initially: single-organ imaging and imaging over several bed positions (e.g. whole- and total-body imaging). Each of the two categories may comprise scans for very different indications; however, patient set-up and imaging order can be similar.

Single-Organ Imaging

Single organ imaging is often performed within one (e.g. for brain) or more than one (e.g. for lungs) bed-positions, depending on the organ size and the scanner's field-of-view (FOV), to study organ function (e.g. brain, heart, liver) or regional disease (e.g. tumour, carotid plaques) in detail. They often require dynamic, gated or longer PET and/or MR acquisitions. Most of the times, MRI requires the longest acquisition times, due to the several pulse sequences and further functional information that may be necessary for a comprehensive diagnosis. In scanners with simultaneous

acquisition capabilities, the required acquisition time for diagnostic MR and the extra sequences required for MR-based PET attenuation correction (MRAC) will define the total acquisition time.

It is common for research brain PET imaging to require dynamic acquisitions for studying tracer kinetics. These are long scans in order to capture both early and late phases of the tracer uptake. In these cases simultaneous PET/MR acquisition is prefered, from the workflow perspective, as MR scans can be acquired at the same time. One example is given in Fig. 3.1 for an application in neuro-oncology [22].

In clinical practice, shorter, static scans are more common. The most predominant brain PET indications include assessment of dementia with FDG or Amyloid imaging, surgical planning for focal epilepsy with FDG and to a lesser extent Parkinson's disease with ^{18}F-DOPA. Neuro-oncology uses tracers for metabolic assessment, receptor imaging and hypoxia as, and in addition to the list in Table 3.1. Most of these scans are static and, although shorter than many dynamic acquisitions, are still longer than the individual bed-position duration in whole-body protocols, requiring still 15-20 min as a crude average. In these cases, diagnostic MR may require longer acquisitions, again due to several different contrasts that may be required. Two generic imaging protocols for such scans are illustrated in Fig. 3.2 for simultaneous and sequential acquisitions. In both cases, the MR scans can start before or after PET depending on the workflow of the department and, in some occasions, MR scans may start during the radiotracer's uptake time [59].

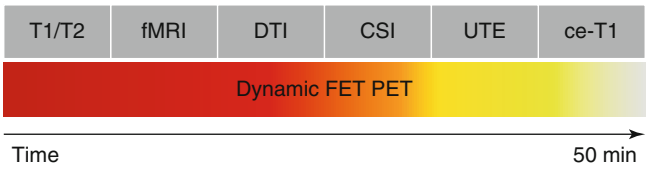

Fig. 3.1 Example protocol for PET/MR scan in neuro-oncology, comprising a dynamic ^{18}F-FET PET and several MR acquisitions, where *CSI* Chemical Shift Imaging, *UTE* Ultra-Short Time Echo, *ce* contrast enhanced scan (Adapted from Neuner et al. [22])

As indicated earlier, another promising area for PET/MR use is in cardiovascular imaging [44]. Imaging of myocardial viability, e.g. after acute myocardial infarction, or identifying vulnerable plaques in the carotid arteries also require single-bed acquisitions. Myocardial imaging often requires motion compensation for heart movement, which is performed through cardiac gating. Such gating in PET/MR can be done either using image-derived information from MRI, to gate both PET and MRI data in a simultaneous acquisition system, or via external triggering of both modalities in sequential acquisition systems. Figure 3.3 illustrates cardiac-gated exams acquired using the two different gating approaches.

Cardiac imaging protocols may have similar forms to those in Fig. 3.2. Depending on the amount and type of MR sequences needed, as well as the scanner's technology, but they are often faster than brain scans. An example of a comprehensive cardiac gated protocol and acquisition times, using a sequential system, is presented in Table 3.2 [59].

Whole-Body Imaging

For whole-body (i.e. eyes-to-thighs) or total-body (i.e. head-to-toes) imaging, several bed positions are acquired and merged. Modern PET systems require between 1 and 3 min per bed position, and the amount of bed positions needed is defined by the length of the required scan and the axial size of PET FOV. The latter in the current PET/MR scanners vary between 18 and 25.8 cm with overlap up to 50 % [60, 61]. On the other hand, diagnostic MR protocols may easily surpass 60 min of total acquisition time. The type of acquisition for both subsystems can vary significantly and, on some occasions, the protocols may need modifications in light of new data arising from one of the two modalities. For example, in a staging examination, both local disease and possible distant metastases, need to be assessed. In that case MRAC/localisation scan, followed by the FDG-PET acquisition is performed first and findings may indicate the distant regions with sus-

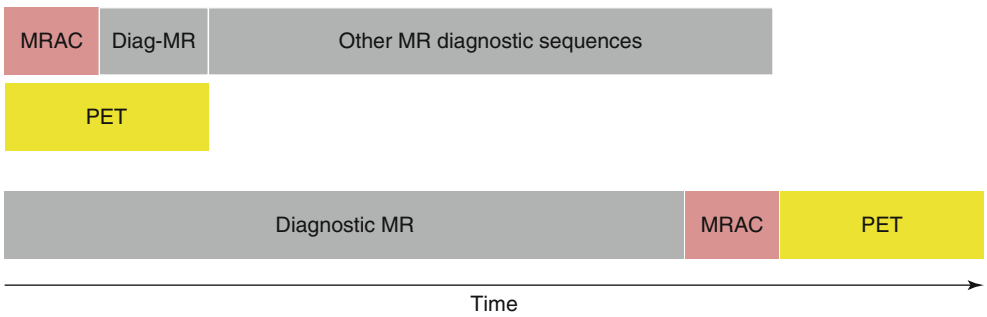

Fig. 3.2 Simultaneous and sequential PET/MR scans for a single-bed/station image acquisition

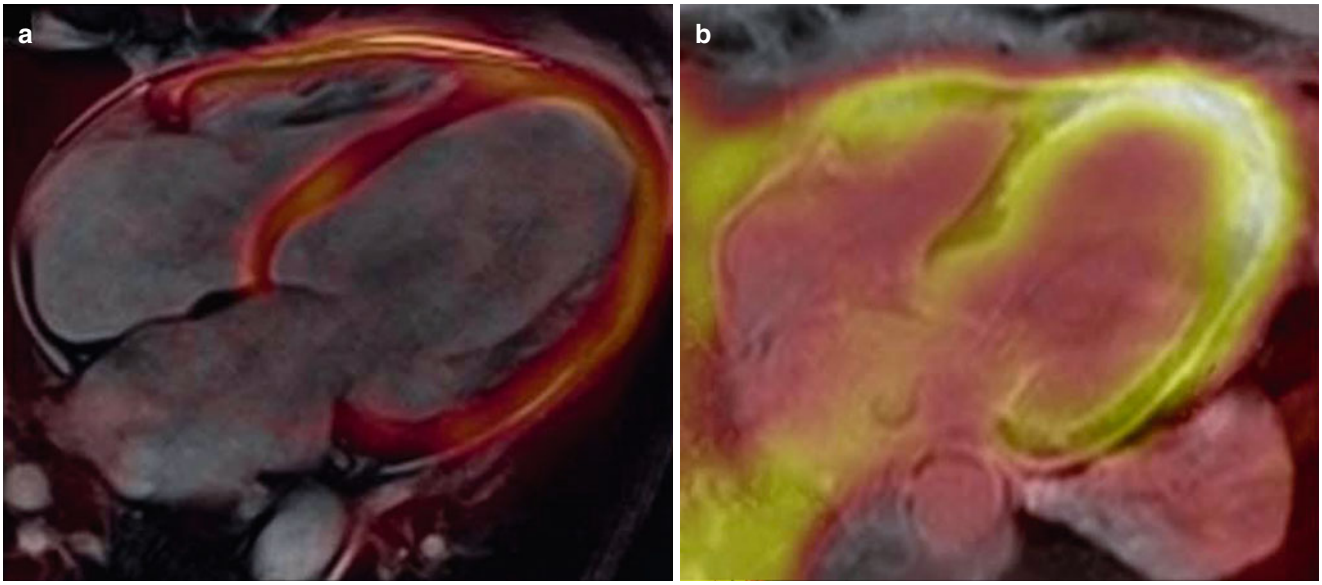

Fig. 3.3 Gated PET/MR studies acquired (**a**) on a simultaneous acquisition system with MR image-derived gating (Image courtesy of Siemens Healthcare) and (**b**) on a sequential acquisition system with independent external ECG triggering (Image courtesy of Dr R Nkoulou & Prof JP Vallée, HUG)

Table 3.2 Comprehensive sequential PET/MR imaging protocol for assessing myocardial viability

Heart protocol	Acq. time (min)	Effective acq. time (min)[a]	Acq. res (mm)	Rec. res. (mm)	TR/TE (ms)
M2D-B-TFE	00:00:09	00:01:00	2.07/1.85/10.0	0.61/0.61/10.0	2.8/1.40
B-TFE 2 chamber (LV)	00:00:09	00:01:00	2.01/1.79/8.00	1.16/1.16/8.00	3.2/1.60
B-TFE 2 chambers (RV)	00:00:11	00:01:00	2.01/1.79/8.00	1.16/1.16/8.00	3.2/1.66
B-TFE 4 chambers	00:00:11	00:01:00	2.01/1.82/8.00	1.16/1.16/8.00	3.3/1.66
B-TFE short axis (×8 to cover all LV)	00:01:15	00:08:00	2.01/1.82/8.00	1.16/1.16/8.00	3.3/1.66
Dynamic sTFE 3 slices	00:00:59	00:00:59	2.98/3.03/10.0	1.28/1.28/10.0	2.5/1.27
PSIR-TFE-2 chambers	00:00:06	00:01:00	1.60/2.29/10.0	0.61/0.61/10.0	6.1/3.0 (TI=90)
PSIR-TFE-4 chambers	00:00:06	00:01:00	1.60/2.29/10.0	0.61/0.61/10.0	6.1/3.0 (TI=90)
PSIR-TFE-short axis	00:00:06	00:01:00	1.60/2.29/10.0	0.61/0.61/10.0	6.1/3.0 (TI=90)
IR-TFE-LL	00:00:10	00:01:00	2.73/2.78/10.0	1.37/1.37/10.0	8.0/3.2
3D-IRTFE 4 chambers	00:00:09	00:01:00	2.01/2.01/10.0	1.16/1.16/5.00	3.5/1.13
3D-IRTFE 2 chambers	00:00:09	00:01:00	2.01/2.01/10.0	1.16/1.16/5.00	3.5/1.13
3D-IRTFE short axis	00:00:09	00:01:00	2.01/2.01/10.0	1.16/1.16/5.00	3.5/1.13
atMR cardiac	00:01:06	00:01:06	3.00/3.00/6.00	1.88/1.88/6.00	4.1/2.3
Gated FDG-PET (10 cardiac phases)	00:10:00	00:10:00		4.00/4.00/4.00	
Total time	**00:14:45**	**00:22:59**			

Courtesy of Prof JP Vallée, Dr R Nkoulou, Prof O Ratib, HUG
In Italics are all the PET/specific components
[a]Counting breathold time and recuperation, each sequence is performed in ~1 min

pected metastasis to be interrogated later on by the localised diagnostic MR contrasts (e.g. in breast cancer staging).

On a PET/MR tomograph with simultaneous acquisition capabilities, PET acquisitions run for 2–6 min per bed position [62, 63] and, during this time, MR also acquires data for MRAC (19 s/bed) as well as other relevant for each examination, sequences. Often, specific body areas require longer MR acquisitions, e.g. for the complete assessment of primary tumours. Depending on the clinical indication, PET tracer and processes of the department, these extra MR sequences can be performed before or after the simultaneous PET/MR acquisition. When the additional MR scans are performed prior to PET/MR acquisition, and for PET agents such as FDG, the patient may be scanned during the uptake period after the tracer injection. For FDG, however, consideration should be given in minimising potential FDG uptake in muscles [64]. Alternatively, when the additional MR scans are performed after simultaneous PET/MR, an additional PET acquisition

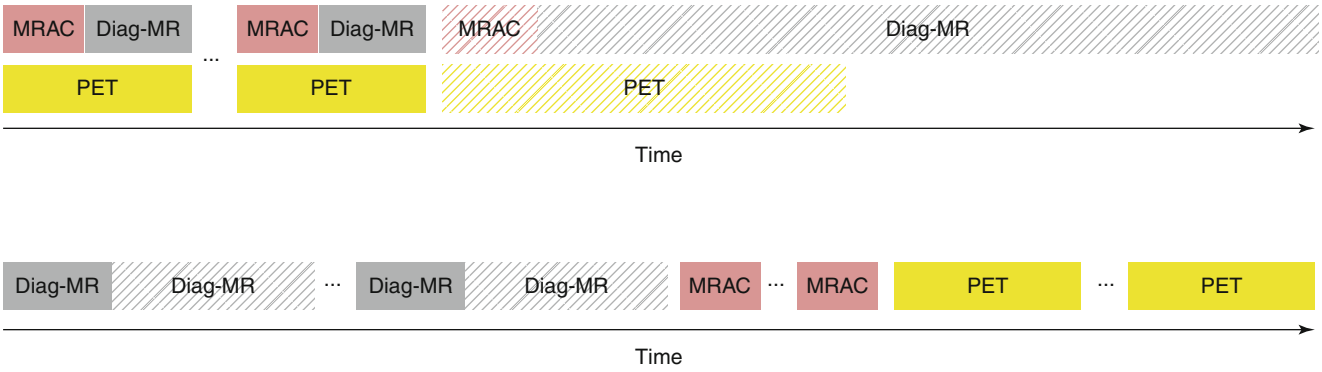

Fig. 3.4 Generalised simultaneous (*top*) and sequential (*bottom*) PET/MR whole-body imaging protocols. Diag-MR and MRAC indicate diagnostic MR acquisitions and MR sequences for attenuation correction and PET localisation, respectively. *Solid bars* indicate the minimum required acquisitions while hatched bars are extra imaging required by specific imaging protocols and their relative positions. The two time axes do not suggest equal acquisition time between the two protocols

can be acquired which can provide dynamic data [62] or a late acquisition which for agents such as FDG it is shown to provide more or different information than early scans [65–68].

On the other hand, in a different scanner with sequential acquisition capabilities, one option would be to perform all the diagnostic MR acquisitions at the beginning, followed by MRAC dedicated sequences and then PET. A clinical indication which would use such a protocol (Fig. 3.4) is to assess response to treatment or in Head/Neck cancer surgery planning [59]. Workflow optimisation is even more necessary for sequential acquisition settings, since the luxury of PET acquisition during MR is not present. Hence, current sequential scanner designs are trying to leverage technologies from both modalities such as Time-of-Flight (TOF) PET and multiple transmission MRI in order to minimise the required imaging time. The MRAC whole-body scan requires approximately 4–6 min [69], while a TOF PET scan is shown to be performed as fast as 30s/bed position [70, 71] but times between 1-2 min/bed are more common. The decision for how long to acquire PET data depends on the site preferences and experience with TOF-PET systems. Examples in literature exist which demonstrate the use of PET with short acquisition protocols for FDG [72] and other radio-tracers [73].

One improvement in the area of high-field MR is brought by the introduction of parallel transmission, which reduces the local Specific Absorption Rate (SAR), resulting in shorter pulse repetition time and, hence, faster acquisitions [74, 75]. Gains in acquisition time, though, vary depending on the pulse sequences used. From comparisons with standard high-field MR in literature it was found to accelerate lumbar spine imaging by 50 % for T2 sagittal and 18 % for T1 sagittal sequences; while in the pelvis, T2 fast spin-echo sequences could be acquired with a time gain of 33 % [76]. Finally, the average expected acquisition time improvement from multi-transmit was found to be 31 % across 77 clinically tested MR sequences [77].

Technical Requirements

The necessary technology for building a PET/MR scanner is already described in detail in a different chapter of this book. The current section attempts to link specific clinical and/or workflow needs for PET/MRI and the main technological requirements which may address these needs. The two main such needs is the reduction of scan time and the equivalence of image quality as well as quantification of PET/MR in comparison with stand-alone MRI and PET/CT.

Scan Time

As it became apparent so far in the discussion, one major consideration is the PET/MR acquisition time. Shorter exam times ensure patient comfort and faster throughput (implying reduced cost per exam). However, faster throughput should be considered together with the fact that radiation exposure to staff might be higher in PET/MR than in PET/CT due to longer patient setting-up times that MRI scans require, and the current lack of formalised reimbursement framework for PET/MR scans. These two parameters may limit anyhow the patient availability per day for PET/MR scans.

On the other hand, both PET and MRI have limitations with respect to their signal detection efficiency. For PET imaging, only a certain amount of radiotracer can be administered according to national and local health and safety regulations, while the tomograph itself has a significantly low detection efficiency, despite its ability for absolute quantification [78]. MRI has also low sensitivity, due to the inherent low macroscopic magnetisation of the human body [79]. Therefore, the longer the acquisition time, the better the quantification and image quality can be achieved by for both modalities.

The scanner design and several technologies can improve the above compromise. From the PET side, the straightforward approach is to increase the solid angle of the detector exposed to radioactivity with direct effect on system sensitivity [80]. This can be achieved by increasing the axial FOV and/or placing the detector closer to the body. This has already been successfully employed by one system design [61]. In the last 6 years, advancements in scintillation crystals, electronics and reconstruction algorithms have enabled PET systems to compute with higher accuracy the origin of each registered event using Time-of-Flight (TOF) and significantly improving the signal-to-noise (SNR) ratio in images [81] at levels higher than expected for the given sensitivity of the scanner [82] and keeping all other imaging parameters equal. This route has also been exploited by another system design [60].

From the MRI side, several techniques have been attempted in order to reduce the acquisition time. Fast pulse sequences have been developed, sometimes at the expense of spatial resolution or SNR [83]. The use of 3T MRI despite its excellent spatial resolution and contrast that introduced it made acquisitions longer due to the need to account for increased levels of local Specific Absorption Rate (SAR) by increasing Repetition Times (TR) in the pulse sequences [84]. Two other MRI technologies, that lead to a reduction in scan time, is parallel acquisition with multiple coil elements [85], and parallel transmission [86]. Parallel acquisition uses multiple receiver coil channels that provide additional spatial information for the reconstruction of the under-sampled K-space in the phase encoding direction [87]. Parallel acquisition algorithms work either with the acquired aliased images (e.g. SENSE [88]) or by reconstructing the missing K-space data (e.g. GRAPPA [89]). A more recent technology, parallel transmission utilizes multiple transmission channels and RF sources to adjust the power, amplitude, phase and waveform for optimal excitation and homogeneous receive fields for each specific patient anatomy [76]. The latter has as a result homogeneous fat suppression [90] and better image quality for difficult regions such as spine [77], breast [91], heart [92] and pelvis [76]. In addition, parallel transmission benefits PET/MR through the reduction of local SAR, allowing for significant increases in scanning speed [76].

Image Quality and Quantification

A major advantage for PET/MR versus MRI is the high specificity of PET as well as its relative and absolute quantification of the radiotracer bio-distribution. This becomes possible after the implementation of several corrections on the PET data related to ionising radiation measurements; namely, radioactive decay, the attenuation and scatter of photons in matter and random registered coincidences

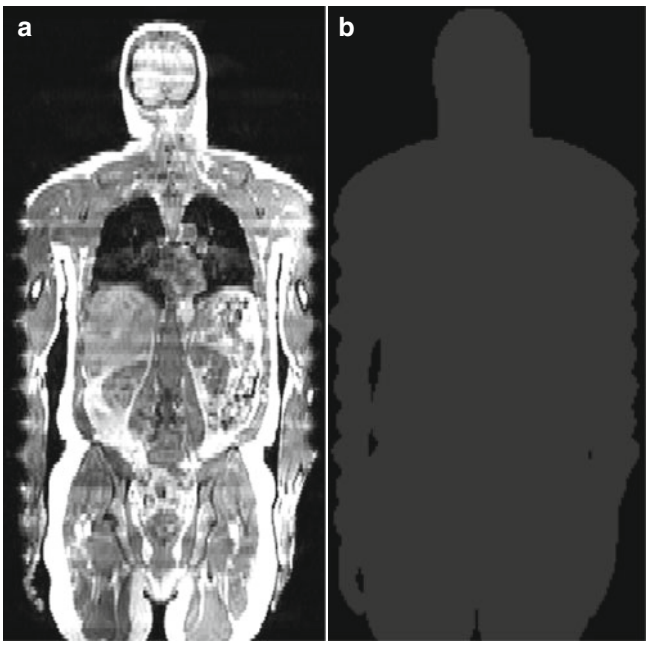

Fig. 3.5 Example of (**a**) the MR FOV truncation, and (**b**) the maximum intensity projection of the resulting MRAC map demonstrating the truncation effect

resulting into faulty estimated events [93]. For PET/MR, most of these corrections are estimated using identical or similar procedures to stand-alone PET and PET/CT. However, this is not true for attenuation correction [94] and scatter correction may also be problematic in certain clinical applications.

Attenuation correction in stand-alone PET is performed by acquiring a transmission scan using rotating ^{68}Ge or ^{137}Cs sources or, in modern PET/CTs, a low-dose CT scan (CTAC) is used (Fig. 2.12). In contrast to CT, MRI does not provide the electron density information of the scanned object, the primary cause of photon attenuation. Therefore, MR images require further manipulation to derive attenuation coefficients. Several MR-based attenuation correction (MRAC) methods exist in literature, based on anatomical atlases [95], segmentation of images obtained with specific MR sequences [96–98] or a combination of both [99]. Two further requirements for such methodology are to use MR images that can be acquired in a clinically feasible time (as a significant amount of PET/MR applications are expected to require whole-body imaging) and are able to provide useful clinical information for whole-body disease assessment. Currently, the methods implemented on the commercial systems use specific MR-sequences and segmentation of three [69] or four [97] different classes of attenuating media.

Another important concern for MRAC is the smaller MRI transverse FOV versus that of PET. This difference frequently results in truncation of hands and shoulders in the MR image of a number of patients (Fig. 3.5a). The result is a truncated MRAC map (Fig. 3.5b) causing bias in

quantification and image artefacts in PET [100, 101]. The currently implemented truncation compensated methods on the two commercial systems use two different approaches. The missing parts of the attenuation maps are estimated in the first case by a modified iterative reconstruction algorithm using the emission PET data [102], while the second utilises an edge-detection algorithm operating on the reconstructed non-attenuated PET image and using prior knowledge of the scanner design [100].

The first implemented MRAC methods do not take into account cortical bone [97, 103], the highest attenuating material in the human body. Although currently published data from both commercially implemented methods do not show any clinically relevant quantitative inaccuracies [69, 97, 104], a different study showed that MRAC without a bone class underestimates SUVs in certain areas such as spine and pelvis [105]. Another study, using CTAC maps processed in such a way to mimic MRAC, found SUV_{mean} underestimated by 11 % for total bone lesions with femur being the highest (17 %) [106]. These findings indicate that, depending on the clinical application, more thorough studies may identify quantification concerns for first generation MRAC methods.

Since the transverse relaxation time (T2) of cortical bone is very short [107], the signal from bone has decayed at the time of image acquisition in classical MR sequences. Thus, a separation of air and bone is not possible on the acquired MR images. To obtain a bone signal, Ultra-short Echo Time (UTE) sequences, in particular, have been used [108, 109] for MR attenuation correction. UTE sequences sample the free induction decay (FID) directly after the excitation of the spins, yielding signal from bone and all other tissue, while an echo signal is acquired in the same sequence, where the bone signal has already decayed. Attenuation maps are then derived by segmenting the images into air, tissue and bone components [59]. Unfortunately, such sequences require long acquisition time [108] while the resulting images do not have clinically relevant information for most examinations. This is an on-going area of research and several academic and industry groups are trying to improve MRAC with clinically sensible MR acquisition times.

Another area of concern regarding MRAC the presence of magnetically susceptible materials (e.g. metal implants or medical devices) in the MR FOV, will result into susceptibility artefacts, i.e. signal void areas and bright signals in the tissues surrounding the implants [110]. Such artefacts propagate in the MRAC map in a relatively arbitrary fashion, depending on the location and extent of the artefact (Fig. 3.6). Metal artefact reduction sequences (MARS) can be used to reduce the size and intensity of susceptibility artefacts from magnetic field distortion [111]. However, currently only manual corrections may be available.

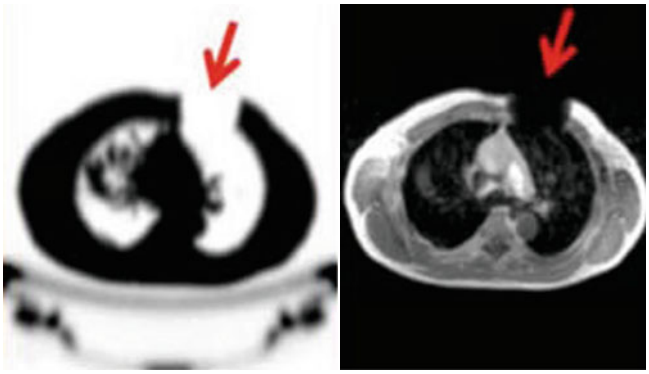

Fig. 3.6 Example of MR artefacts in the acquired image due a cardiac stent, as propagated in the MRAC (Image courtesy of Philips Healthcare)

Apart from attenuation correction, scatter correction may also need some consideration in PET/MR. Although the standard methodology performs very well for most clinical situations, on certain clinical settings when patient set-up may differ from PET/CT, this difference may impact on scatter correction accuracy. For example, in breast cancer, MR patient set-up is different from PET/CT, prone vs. supine positioning, respectively. The main benefit for prone imaging is that the breast tissues are extended by gravity providing higher spatial resolution than in supine position. When prone positioning is selected in PET/MR, occasionally certain parts of the body exhibit extremely low radiotracer uptake, such as the area behind the breast. This causes the scatter correction to fail, impacting both image quality and quantification. To address the incorporation of a priori information from the MR scan in the scatter correction has been investigated [112]. One such example is illustrated in Fig. 3.7.

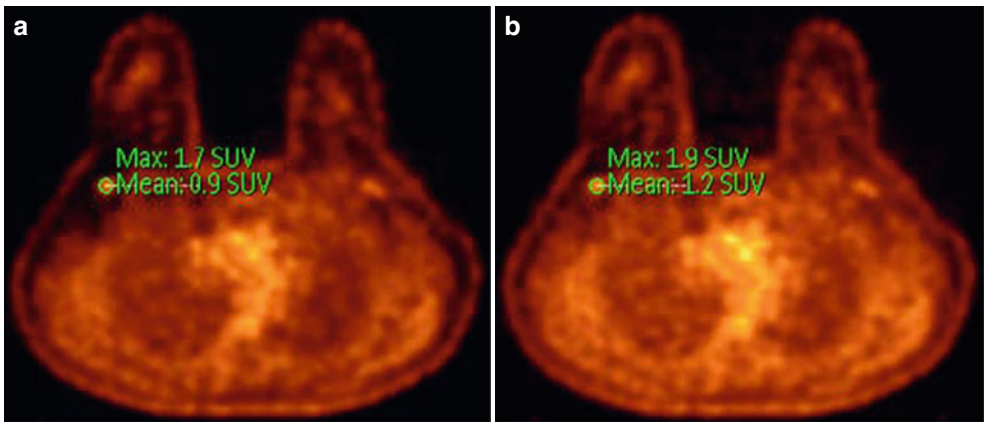

Fig. 3.7 FDG-PET image of a patient in prone position with scatter artefacts impacting on the image quality and quantification in the area behind the right breast (**a**). The same PET image with a modified scatter correction, incorporating information from the MR scan, shows higher SUV uptake, but not enough to indicate malignancy, and higher consistency with the background contrast (**b**) (Images from Kalemis et al. [59])

Conclusions

This chapter has presented generic forms of PET/MR protocols, as been reported by users in literature, and the impact that current technologies have on such imaging protocols. By the time this book was published, whole-body PET/MR had already been in the clinic for two and a half years. During this period a lot of effort was devoted into proving that the new modality performs equally well with stand-alone modalities and PET/CT. For most cases this is already proven but efforts are still underway for improving technologies such as MR-based attenuation correction and motion correction/compensation. The clinical exposure of PET/MR identifies important areas for improvement and accordingly, technology is still expected to improve in capabilities and performance, and system designs to mature. Judging from PET/CT, most probably we are still several years away from fully-optimised technologies.

Although, the period where image quality comparison between PET/CT vs. PET/MR slowly comes to an end and the next phase of investigating the clinical benefits of the new technology has already started. The optimisation of imaging protocols is an inherent part of streamlining workflows and improving the acquisition of diagnostic information and a two-way impact is expected between the implementation of novel technology and testing of new imaging protocols. Even preliminary results from this phase are of paramount importance for the establishment and acceptance rate of the new modality. Obviously, only time can tell the future of PET/MR; however, judging from the interest, motivation and the investment already made for this novel imaging technology one may say that its chances are quite high. The following chapters will give an idea of future PET/MR clinical applications.

References

1. Ratib O, Beyer T (2011) Whole-body hybrid PET/MRI: ready for clinical use? Eur J Nucl Med Mol Imaging 38(6):992–995
2. Jones T (2002) Molecular imaging with PET – the future challenges. Br J Radiol 75 Spec No:S6–S15
3. Pichler BJ, Kolb A, Nagele T, Schlemmer HP (2010) PET/MRI: paving the way for the next generation of clinical multimodality imaging applications. J Nucl Med 51(3):333–336
4. Schiepers C, Dahlbom M (2011) Molecular imaging in oncology: the acceptance of PET/CT and the emergence of MR/PET imaging. Eur Radiol 21(3):548–554
5. Zaidi H, Del Guerra A (2011) An outlook on future design of hybrid PET/MRI systems. Med Phys 38(10):5667–5689
6. Kielstra P (2009) Doctor innovation: shaking up the health system. The Economist Intelligence Unit, London
7. Oates ME, Diagnostic Radiology Participants of ACRSNMTF, II (2012) Integrated residency training pathways of the future: diagnostic radiology, nuclear radiology, nuclear medicine, and molecular imaging. J Am Coll Radiol 9(4):239–244
8. Bolus NE, George R, Washington J, Newcomer BR (2009) PET/MRI: the blended-modality choice of the future? J Nucl Med Technol 37(2):63–71; quiz 72–63
9. Hicks RJ, Lau EW (2009) PET/MRI: a different spin from under the rim. Eur J Nucl Med Mol Imaging 36(Suppl 1):S10–S14
10. Goyen M, Debatin JF (2009) Healthcare costs for new technologies. Eur J Nucl Med Mol Imaging 36(Suppl 1):S139–S143
11. von Schulthess GK, Schlemmer HP (2009) A look ahead: PET/MR versus PET/CT. Eur J Nucl Med Mol Imaging 36(Suppl 1):S3–S9
12. Heiss WD (2009) The potential of PET/MR for brain imaging. Eur J Nucl Med Mol Imaging 36(Suppl 1):S105–S112
13. Saraste A, Knuuti J (2012) Cardiac PET, CT, and MR: what are the advantages of hybrid imaging? Curr Cardiol Rep 14(1):24–31
14. Herzog H, Langen K-J, Kaffanke J, Weirich C, Neuner I, Stoffels G, Kops ER, Scheins J, Tellmann L, Shah NJ (2010) MR-PET opens new horizons in neuroimaging. Future Neurol 5(6):807–815
15. Jansen NL, Graute V, Armbruster L, Suchorska B, Lutz J, Eigenbrod S, Cumming P, Bartenstein P, Tonn JC, Kreth FW, la Fougere C (2012) MRI-suspected low-grade glioma: is there a need to perform dynamic FET PET? Eur J Nucl Med Mol Imaging 39(6):1021–1029
16. Beuthien-Baumann B, Platzek I, Lauterbach I, van den Hoff J, Schramm G, Zophel K, Laniado M, Kotzerke J (2012) Improved anatomic visualization of a glomus caroticum tumour within the carotic bifurcation with combined 68 Ga-DOTATATE PET/MRI. Eur J Nucl Med Mol Imaging 39(6):1087–1088

17. Cui J, Pratx G, Prevrhal S, Zhang B, Shao L, Levin CS (2011) Measurement-based spatially-varying point spread function for list-mode PET reconstruction on GPU. In: IEEE nuclear science symposium and medical imaging conference (NSS/MIC), 2011 IEEE, 23–29 Oct 2011, Valencia, pp 2593–2596
18. Panin VY, Kehren F, Rothfuss H, Hu D, Michel C, Casey ME (2006) PET reconstruction with system matrix derived from point source measurements. Nucl Sci IEEE Trans 53(1):152–159
19. Schwenzer NF, Stegger L, Bisdas S, Schraml C, Kolb A, Boss A, Muller M, Reimold M, Ernemann U, Claussen CD, Pfannenberg C, Schmidt H (2012) Simultaneous PET/MR imaging in a human brain PET/MR system in 50 patients – current state of image quality. Eur J Radiol. doi:10.1016/j.ejrad.2011.12.027
20. Boss A, Bisdas S, Kolb A, Hofmann M, Ernemann U, Claussen CD, Pfannenberg C, Pichler BJ, Reimold M, Stegger L (2010) Hybrid PET/MRI of intracranial masses: initial experiences and comparison to PET/CT. J Nucl Med 51(8):1198–1205
21. Boss A, Kolb A, Hofmann M, Bisdas S, Nagele T, Ernemann U, Stegger L, Rossi C, Schlemmer HP, Pfannenberg C, Reimold M, Claussen CD, Pichler BJ, Klose U (2010) Diffusion tensor imaging in a human PET/MR hybrid system. Invest Radiol 45(5):270–274
22. Neuner I, Kaffanke JB, Langen KJ, Kops ER, Tellmann L, Stoffels G, Weirich C, Filss C, Scheins J, Herzog H, Shah NJ (2012) Multimodal imaging utilising integrated MR-PET for human brain tumour assessment. Eur Radiol 22(12):2568–2580
23. Arbizu J, Tejada S, Marti-Climent JM, Diez-Valle R, Prieto E, Quincoces G, Vigil C, Idoate MA, Zubieta JL, Penuelas I, Richter JA (2012) Quantitative volumetric analysis of gliomas with sequential MRI and (11)C-methionine PET assessment: patterns of integration in therapy planning. Eur J Nucl Med Mol Imaging 39(5):771–781
24. Heinzel A, Stock S, Langen K-J, Müller D (2012) Cost-effectiveness analysis of FET PET/guided target selection for the diagnosis of gliomas. Eur J Nucl Med Mol Imaging 39(7):1089–1096
25. Takenaka S, Shinoda J, Asano Y, Aki T, Miwa K, Ito T, Yokoyama K, Iwama T (2011) Metabolic assessment of monofocal acute inflammatory demyelination using MR spectroscopy and (11) C-methionine-, (11)C-choline-, and (18)F-fluorodeoxyglucose-PET. Brain Tumor Pathol 28(3):229–238
26. Galldiks N, Langen KJ, Holy R, Pinkawa M, Stoffels G, Nolte KW, Kaiser HJ, Filss CP, Fink GR, Coenen HH, Eble MJ, Piroth MD (2012) Assessment of treatment response in patients with glioblastoma using O-(2-18F-fluoroethyl)-L-tyrosine PET in comparison to MRI. J Nucl Med 53(7):1048–1057
27. Thorwarth D, Henke G, Muller AC, Reimold M, Beyer T, Boss A, Kolb A, Pichler B, Pfannenberg C (2011) Simultaneous 68Ga-DOTATOC-PET/MRI for IMRT treatment planning for meningioma: first experience. Int J Radiat Oncol Biol Phys 81(1):277–283
28. Pirotte B, Goldman S, Dewitte O, Massager N, Wikler D, Lefranc F, Ben Taib NO, Rorive S, David P, Brotchi J, Levivier M (2006) Integrated positron emission tomography and magnetic resonance imaging-guided resection of brain tumors: a report of 103 consecutive procedures. J Neurosurg 104(2):238–253
29. Pirotte B, Goldman S, Van Bogaert P, David P, Wikler D, Rorive S, Brotchi J, Levivier M (2005) Integration of [11C]methionine-positron emission tomographic and magnetic resonance imaging for image-guided surgical resection of infiltrative low-grade brain tumors in children. Neurosurgery 57(1 Suppl):128–139; discussion 128–139
30. Garibotto V, Vargas MI, Lovblad KO, Ratib O (2011) A PET/MRI case of corticocerebellar diaschisis after stroke. Clin Nucl Med 36(9):821–825
31. Brockmann K, Reimold M, Globas C, Hauser TK, Walter U, Machulla HJ, Rolfs A, Schols L (2012) PET and MRI reveal early evidence of neurodegeneration in spinocerebellar ataxia type 17. J Nucl Med 53(7):1074–1080
32. Drzezga A, Becker JA, Van Dijk KR, Sreenivasan A, Talukdar T, Sullivan C, Schultz AP, Sepulcre J, Putcha D, Greve D, Johnson KA, Sperling RA (2011) Neuronal dysfunction and disconnection of cortical hubs in non-demented subjects with elevated amyloid burden. Brain 134(Pt 6):1635–1646
33. Kanda T, Ishii K, Uemura T, Miyamoto N, Yoshikawa T, Kono AK, Mori E (2008) Comparison of grey matter and metabolic reductions in frontotemporal dementia using FDG-PET and voxel-based morphometric MR studies. Eur J Nucl Med Mol Imaging 35(12):2227–2234
34. Karow DS, McEvoy LK, Fennema-Notestine C, Hagler DJ Jr, Jennings RG, Brewer JB, Hoh CK, Dale AM, Alzheimer's Disease Neuroimaging I (2010) Relative capability of MR imaging and FDG PET to depict changes associated with prodromal and early Alzheimer disease. Radiology 256(3):932–942
35. Brodbeck V, Spinelli L, Lascano AM, Wissmeier M, Vargas M-I, Vulliemoz S, Pollo C, Schaller K, Michel CM, Seeck M (2011) Electroencephalographic source imaging: a prospective study of 152 operated epileptic patients. Brain 134(10):2887–2897
36. Carne R, O'Brien T, Kilpatrick C, MacGregor L, Litewka L, Hicks R, Cook M (2007) 'MRI-negative PET/positive' temporal lobe epilepsy (TLE) and mesial TLE differ with quantitative MRI and PET: a case control study. BMC Neurol 7(1):16
37. Rubi S, Setoain X, Donaire A, Bargallo N, Sanmarti F, Carreno M, Rumia J, Calvo A, Aparicio J, Campistol J, Pons F (2011) Validation of FDG-PET/MRI coregistration in nonlesional refractory childhood epilepsy. Epilepsia 52(12):2216–2224
38. Buchsbaum MS, Buchsbaum BR, Hazlett EA, Haznedar MM, Newmark R, Tang CY, Hof PR (2007) Relative glucose metabolic rate higher in white matter in patients with schizophrenia. Am J Psychiatry 164(7):1072–1081
39. Buchsbaum MS, Haznedar MM, Aronowitz J, Brickman AM, Newmark RE, Bloom R, Brand J, Goldstein KE, Heath D, Starson M, Hazlett EA (2007) FDG-PET in never-previously medicated psychotic adolescents treated with olanzapine or haloperidol. Schizophr Res 94(1–3):293–305
40. Chang L, Alicata D, Ernst T, Volkow N (2007) Structural and metabolic brain changes in the striatum associated with methamphetamine abuse. Addiction 102(Suppl 1):16–32
41. Haznedar MM, Buchsbaum MS, Hazlett EA, LiCalzi EM, Cartwright C, Hollander E (2006) Volumetric analysis and three-dimensional glucose metabolic mapping of the striatum and thalamus in patients with autism spectrum disorders. Am J Psychiatry 163(7):1252–1263
42. Uttner I, Mottaghy FM, Schreiber H, Riecker A, Ludolph AC, Kassubek J (2006) Primary progressive aphasia accompanied by environmental sound agnosia: a neuropsychological, MRI and PET study. Psychiatry Res 146(2):191–197
43. Versijpt J, Debruyne JC, Van Laere KJ, De Vos F, Keppens J, Strijckmans K, Achten E, Slegers G, Dierckx RA, Korf J, De Reuck JL (2005) Microglial imaging with positron emission tomography and atrophy measurements with magnetic resonance imaging in multiple sclerosis: a correlative study. Mult Scler 11(2): 127–134
44. Nekolla SG, Martinez-Moeller A, Saraste A (2009) PET and MRI in cardiac imaging: from validation studies to integrated applications. Eur J Nucl Med Mol Imaging 36(Suppl 1):S121–S130
45. Knaapen P, Gotte MJ, Paulus WJ, Zwanenburg JJ, Dijkmans PA, Boellaard R, Marcus JT, Twisk JW, Visser CA, van Rossum AC, Lammertsma AA, Visser FC (2006) Does myocardial fibrosis hinder contractile function and perfusion in idiopathic dilated cardiomyopathy? PET and MR imaging study. Radiology 240(2): 380–388
46. Slart R, Glauche J, Golestani R, Zeebregts C, Jansen J, Dierckx R, Oudkerk M, Willems T, Glaudemans A, Boersma H, Tio R (2012) PET and MRI for the evaluation of regional myocardial perfusion

and wall thickening after myocardial infarction. Eur J Nucl Med Mol Imaging 39(6):1065–1069
47. Qiao H, Zhang H, Zheng Y, Ponde DE, Shen D, Gao F, Bakken AB, Schmitz A, Kung HF, Ferrari VA, Zhou R (2009) Embryonic stem cell grafting in normal and infarcted myocardium: serial assessment with MR imaging and PET dual detection. Radiology 250(3):821–829
48. Wu YW, Tadamura E, Yamamuro M, Kanao S, Marui A, Tanabara K, Komeda M, Togashi K (2007) Comparison of contrast-enhanced MRI with (18)F-FDG PET/201Tl SPECT in dysfunctional myocardium: relation to early functional outcome after surgical revascularization in chronic ischemic heart disease. J Nucl Med 48(7): 1096–1103
49. Tang TY, Moustafa RR, Howarth SP, Walsh SR, Boyle JR, Li ZY, Baron JC, Gillard JH, Warburton EA (2008) Combined PET/FDG and USPIO-enhanced MR imaging in patients with symptomatic moderate carotid artery stenosis. Eur J Vasc Endovasc Surg 36(1):53–55
50. Antoch G, Bockisch A (2009) Combined PET/MRI: a new dimension in whole-body oncology imaging? Eur J Nucl Med Mol Imaging 36(Suppl 1):S113–S120
51. Drzezga A, Souvatzoglou M, Eiber M, Beer AJ, Furst S, Martinez-Moller A, Nekolla SG, Ziegler S, Ganter C, Rummeny EJ, Schwaiger M (2012) First clinical experience with integrated whole-body PET/MR: comparison to PET/CT in patients with oncologic diagnoses. J Nucl Med 53(6):845–855
52. Boss A, Stegger L, Bisdas S, Kolb A, Schwenzer N, Pfister M, Claussen CD, Pichler BJ, Pfannenberg C (2011) Feasibility of simultaneous PET/MR imaging in the head and upper neck area. Eur Radiol 21(7):1439–1446
53. Schwenzer NF, Schraml C, Muller M, Brendle C, Sauter A, Spengler W, Pfannenberg AC, Claussen CD, Schmidt H (2012) Pulmonary lesion assessment: comparison of whole-body hybrid MR/PET and PET/CT imaging – pilot study. Radiology 264(2):551–558
54. Lord M, Ratib O, Vallee JP (2011) (1)F-Fluorocholine integrated PET/MRI for the initial staging of prostate cancer. Eur J Nucl Med Mol Imaging 38(12):2288
55. Takei T, Souvatzoglou M, Beer AJ, Drzezga A, Ziegler S, Rummeny EJ, Schwaiger M, Eiber M (2012) A case of multimodality multiparametric 11C-choline PET/MR for biopsy targeting in prior biopsy-negative primary prostate cancer. Clin Nucl Med 37(9):918–919
56. Wissmeyer M, Heinzer S, Majno P, Buchegger F, Zaidi H, Garibotto V, Viallon M, Becker CD, Ratib O, Terraz S (2011) ^{90}Y Time-of-flight PET/MR on a hybrid scanner following liver radioembolisation (SIRT). Eur J Nucl Med Mol Imaging 38(9):1744–1745
57. Buchbender C, Heusner TA, Lauenstein TC, Bockisch A, Antoch G (2012) Oncologic PET/MRI, part 1: tumors of the brain, head and neck, chest, abdomen, and pelvis. J Nucl Med 53(6):928–938
58. Buchbender C, Heusner TA, Lauenstein TC, Bockisch A, Antoch G (2012) Oncologic PET/MRI, part 2: bone tumors, soft-tissue tumors, melanoma, and lymphoma. J Nucl Med 53(8):1244–1252
59. Kalemis A, Delattre BM, Heinzer S (2013) Sequential whole-body PET/MR scanner: concept, clinical use, and optimisation after two years in the clinic. The manufacturer's perspective. MAGMA 26(1):5–23
60. Zaidi H, Ojha N, Morich M, Griesmer J, Hu Z, Maniawski P, Ratib O, Izquierdo-Garcia D, Fayad ZA, Shao L (2011) Design and performance evaluation of a whole-body Ingenuity TF PET/MRI system. Phys Med Biol 56(10):3091–3106
61. Delso G, Furst S, Jakoby B, Ladebeck R, Ganter C, Nekolla SG, Schwaiger M, Ziegler SI (2011) Performance measurements of the Siemens mMR integrated whole-body PET/MR scanner. J Nucl Med 52(12):1914–1922
62. Martinez-Moller A, Eiber M, Nekolla SG, Souvatzoglou M, Drzezga A, Ziegler S, Rummeny EJ, Schwaiger M, Beer AJ (2012) Workflow and scan protocol considerations for integrated whole-body PET/MRI in oncology. J Nucl Med 53(9):1415–1426
63. Werner MK, Schmidt H, Schwenzer NF (2012) MR/PET: a new challenge in hybrid imaging. AJR Am J Roentgenol 199(2):272–277
64. Boellaard R, O'Doherty MJ, Weber WA, Mottaghy FM, Lonsdale MN, Stroobants SG, Oyen WJ, Kotzerke J, Hoekstra OS, Pruim J, Marsden PK, Tatsch K, Hoekstra CJ, Visser EP, Arends B, Verzijlbergen FJ, Zijlstra JM, Comans EF, Lammertsma AA, Paans AM, Willemsen AT, Beyer T, Bockisch A, Schaefer-Prokop C, Delbeke D, Baum RP, Chiti A, Krause BJ (2010) FDG PET and PET/CT: EANM procedure guidelines for tumour PET imaging: version 1.0. Eur J Nucl Med Mol Imaging 37(1):181–200
65. Hamada K, Tomita Y, Qiu Y, Tomoeda M, Ueda T, Tamai N, Hashimoto N, Yoshikawa H, Aozasa K, Hatazawa J (2009) (18) F-FDG PET analysis of schwannoma: increase of SUVmax in the delayed scan is correlated with elevated VEGF/VPF expression in the tumors. Skeletal Radiol 38(3):261–266
66. Chen YM, Huang G, Sun XG, Liu JJ, Chen T, Shi YP, Wan LR (2008) Optimizing delayed scan time for FDG PET: comparison of the early and late delayed scan. Nucl Med Commun 29(5):425–430
67. Nakamoto Y, Higashi T, Sakahara H, Tamaki N, Kogire M, Doi R, Hosotani R, Imamura M, Konishi J (2000) Delayed (18)F-fluoro-2-deoxy-D-glucose positron emission tomography scan for differentiation between malignant and benign lesions in the pancreas. Cancer 89(12):2547–2554
68. Laffon E, de Clermont H, Vernejoux JM, Jougon J, Marthan R (2011) Feasibility of assessing [(18)F]FDG lung metabolism with late dynamic PET imaging. Mol Imaging Biol 13(2):378–384
69. Schulz V, Torres-Espallardo I, Renisch S, Hu Z, Ojha N, Bornert P, Perkuhn M, Niendorf T, Schafer WM, Brockmann H, Krohn T, Buhl A, Gunther RW, Mottaghy FM, Krombach GA (2011) Automatic, three-segment, MR-based attenuation correction for whole-body PET/MR data. Eur J Nucl Med Mol Imaging 38(1):138–152
70. Murray I, Kalemis A, Glennon J, Hasan S, Quraishi S, Beyer T, Avril N (2010) Time-of-flight PET/CT using low-activity protocols: potential implications for cancer therapy monitoring. Eur J Nucl Med Mol Imaging 37(9):1643–1653
71. Conti M (2011) Focus on time-of-flight PET: the benefits of improved time resolution. Eur J Nucl Med Mol Imaging 38(6):1147–1157
72. Derlin T, Weber C, Habermann CR, Herrmann J, Wisotzki C, Ayuk F, Wolschke C, Klutmann S, Kroger N (2012) 18F-FDG PET/CT for detection and localization of residual or recurrent disease in patients with multiple myeloma after stem cell transplantation. Eur J Nucl Med Mol Imaging 39(3):493–500
73. Derlin T, Toth Z, Papp L, Wisotzki C, Apostolova I, Habermann CR, Mester J, Klutmann S (2011) Correlation of inflammation assessed by 18F-FDG PET, active mineral deposition assessed by 18F-fluoride PET, and vascular calcification in atherosclerotic plaque: a dual-tracer PET/CT study. J Nucl Med 52(7):1020–1027
74. Zhu Y (2004) Parallel excitation with an array of transmit coils. Magn Reson Med 51(4):775–784
75. Harvey PR, Zhai Z, Morich M, Mens G, van Yperen G, DeMeester G, Graesslin I, Hoogeveen R (2009) SAR behavior during whole-body multitransmit RF shimming at 3.0T. In: Proceedings of the 17th scientific meeting, International Society for Magnetic Resonance in Medicine, Honolulu, 2009, p 4786
76. Willinek WA, Gieseke J, Kukuk GM, Nelles M, Konig R, Morakkabati-Spitz N, Traber F, Thomas D, Kuhl CK, Schild HH (2010) Dual-source parallel radiofrequency excitation body MR imaging compared with standard MR imaging at 3.0 T: initial clinical experience. Radiology 256(3):966–975
77. Nelles M, Konig RS, Gieseke J, Guerand-van Battum MM, Kukuk GM, Schild HH, Willinek WA (2010) Dual-source parallel RF transmission for clinical MR imaging of the spine at 3.0 T: intraindividual comparison with conventional single-source transmission. Radiology 257(3):743–753
78. Bailey DL (2003) Date acquisition and performance characterization in PET. In: Valk PE, Bailey DL, Townsend DW, Maisey MN

(eds) Positron emission tomography; basic science and clinical practice, 2nd edn. Springer, London, pp 69–90
79. Brix G (2008) Physical basics. In: Reiser MF, Semmler W, Hricak H (eds) Magnetic resonance tomography. Springer, Berlin, pp 8–25
80. Budinger TF (1998) PET instrumentation: what are the limits? Semin Nucl Med 28(3):247–267
81. El Fakhri G, Surti S, Trott CM, Scheuermann J, Karp JS (2011) Improvement in lesion detection with whole-body oncologic time-of-flight PET. J Nucl Med 52(3):347–353
82. Budinger TF (1983) Time-of-flight positron emission tomography: status relative to conventional PET. J Nucl Med 24(1):73–78
83. Blake MA, Hochman MG, Edelman R (2003) Basic principles of MRI including fast imaging. In: Zlatkin MB (ed) MRI of the shoulder, 2nd edn. Lippingcott Williams & Wilkins, Philadelphia
84. DeLano MC, Fisher C (2006) 3T MR imaging of the brain. Magn Reson Imaging Clin N Am 14(1):77–88
85. Pruessmann KP (2006) Encoding and reconstruction in parallel MRI. NMR Biomed 19(3):288–299
86. Katscher U, Börnert P, Leussler C, van den Brink JS (2003) Transmit SENSE. Magn Reson Med 49(1):144–150
87. Deshmane A, Gulani V, Griswold MA, Seiberlich N (2012) Parallel MR imaging. J Magn Reson Imaging 36(1):55–72
88. Pruessmann KP, Weiger M, Scheidegger MB, Boesiger P (1999) SENSE: sensitivity encoding for fast MRI. Magn Reson Med 42(5):952–962
89. Griswold MA, Jakob PM, Heidemann RM, Nittka M, Jellus V, Wang J, Kiefer B, Haase A (2002) Generalized autocalibrating partially parallel acquisitions (GRAPPA). Magn Reson Med 47(6):1202–1210
90. Heilman JA, Derakhshan JD, Riffe MJ, Gudino N, Tkach J, Flask CA, Duerk JL, Griswold MA (2012) Parallel excitation for B-field insensitive fat-saturation preparation. Magn Reson Med. doi:10.1002/mrm.23238
91. Rahbar H, Partridge SC, Demartini WB, Gutierrez RL, Parsian S, Lehman CD (2012) Improved B(1) homogeneity of 3 tesla breast MRI using dual-source parallel radiofrequency excitation. J Magn Reson Imaging 35(5):1222–1226
92. Mueller A, Kouwenhoven M, Naehle CP, Gieseke J, Strach K, Willinek WA, Schild HH, Thomas D (2012) Dual-source radiofrequency transmission with patient-adaptive local radiofrequency shimming for 3.0-T cardiac MR imaging: initial experience. Radiology 263(1):77–85
93. Bailey DL, Karp JS, Surti S (2003) Physics and instrumentation in PET. In: Valk PE, Bailey DL, Townsend DW, Maisey MN (eds) Positron emission tomography; basic science and clinical practice, 2nd edn. Springer, London, pp 41–67
94. Hofmann M, Pichler B, Scholkopf B, Beyer T (2009) Towards quantitative PET/MRI: a review of MR-based attenuation correction techniques. Eur J Nucl Med Mol Imaging 36(Suppl 1): S93–S104
95. Schreibmann E, Nye JA, Schuster DM, Martin DR, Votaw J, Fox T (2010) MR-based attenuation correction for hybrid PET/MR brain imaging systems using deformable image registration. Med Phys 37(5):2101–2109
96. Keereman V, Vandenberghe S, De Deene Y, Luypaert R, Broux T, Lemahieu I (2008) MR-based attenuation correction for PET using an Ultrashort Echo Time (UTE) sequence. In: IEEE nuclear science symposium conference record, Dresden, 19–25 Oct 2008, pp 4656–4661
97. Martinez-Moller A, Souvatzoglou M, Delso G, Bundschuh RA, Chefd'hotel C, Ziegler SI, Navab N, Schwaiger M, Nekolla SG (2009) Tissue classification as a potential approach for attenuation correction in whole-body PET/MRI: evaluation with PET/CT data. J Nucl Med 50(4):520–526
98. Johansson A, Karlsson M, Nyholm T (2011) CT substitute derived from MRI sequences with ultrashort echo time. Med Phys 38(5):2708–2714
99. Hofmann M, Steinke F, Scheel V, Charpiat G, Farquhar J, Aschoff P, Brady M, Scholkopf B, Pichler BJ (2008) MRI-based attenuation correction for PET/MRI: a novel approach combining pattern recognition and atlas registration. J Nucl Med 49(11):1875–1883
100. Hu Z, Renisch S, Schweizer B, Blaffert T, Ojha N, Guo T, Tang J, Tung C, Kaste J, Schulz V, Torres I, Shao L (2010) MR-based attenuation correction for whole-body PET/MR system. In: IEEE nuclear science symposium conference record (NSS/MIC), Knoxville, 30 Oct–6 Nov 2010, pp 2119–2122
101. Delso G, Martinez-Moller A, Bundschuh RA, Nekolla SG, Ziegler SI (2010) The effect of limited MR field of view in MR/PET attenuation correction. Med Phys 37(6):2804–2812
102. Nuyts J, Michel C, Fenchel M, Bal G, Watson C (2010) Completion of a truncated attenuation image from the attenuated PET emission data. In: Nuclear science symposium conference record (NSS/MIC), 2010 IEEE, Knoxville, 30 Oct–6 Nov 2010, pp 2123–2127
103. Hu Z, Ojha N, Renisch S, Schulz V, Torres I, Buhl A, Pal D, Muswick G, Penatzer J, Guo T, Bönert P, Tung C, Kaste J, Morich M, HAVENS T, Maniawski P, Schäfer W, Günther RW, Krombach GA, Shao L (2009) MR-based attenuation correction for a whole-body sequential PET/MR system. In: IEEE nuclear science symposium conference record (NSS/MIC), Orlando, pp 3508–3512
104. Eiber M, Martinez-Moller A, Souvatzoglou M, Holzapfel K, Pickhard A, Loffelbein D, Santi I, Rummeny EJ, Ziegler S, Schwaiger M, Nekolla SG, Beer AJ (2011) Value of a Dixon-based MR/PET attenuation correction sequence for the localization and evaluation of PET/positive lesions. Eur J Nucl Med Mol Imaging 38(9):1691–1701
105. Hofmann M, Bezrukov I, Mantlik F, Aschoff P, Steinke F, Beyer T, Pichler BJ, Scholkopf B (2011) MRI-based attenuation correction for whole-body PET/MRI: quantitative evaluation of segmentation- and atlas-based methods. J Nucl Med 52(9):1392–1399
106. Samarin A, Burger C, Wollenweber SD, Crook DW, Burger IA, Schmid DT, von Schulthess GK, Kuhn FP (2012) PET/MR imaging of bone lesions – implications for PET quantification from imperfect attenuation correction. Eur J Nucl Med Mol Imaging 39(7):1154–1160
107. Du J, Hamilton G, Takahashi A, Bydder M, Chung CB (2007) Ultrashort echo time spectroscopic imaging (UTESI) of cortical bone. Magn Reson Med 58(5):1001–1009
108. Keereman V, Fierens Y, Broux T, De Deene Y, Lonneux M, Vandenberghe S (2010) MRI-based attenuation correction for PET/MRI using ultrashort echo time sequences. J Nucl Med 51(5):812–818
109. Catana C, van der Kouwe A, Benner T, Michel CJ, Hamm M, Fenchel M, Fischl B, Rosen B, Schmand M, Sorensen AG (2010) Toward implementing an MRI-based PET attenuation-correction method for neurologic studies on the MR-PET brain prototype. J Nucl Med 51(9):1431–1438
110. Bagheri MH, Hosseini MM, Emami MJ, Foroughi AA (2012) Metallic artifact in MRI after removal of orthopedic implants. Eur J Radiol 81(3):584–590
111. Olsen RV, Munk PL, Lee MJ, Janzen DL, MacKay AL, Xiang QS, Masri B (2000) Metal artifact reduction sequence: early clinical applications. Radiographics 20(3):699–712
112. Hu Z, Ye J, Hsieh Y-L, Renisch S, Blaffert T, Heinzer S, Loubeyre P, Maniawski P, Shao L, Ratib O (2012) Technical optimization of breast imaging on a combined PET/MR system. J Nucl Med Meet Abstr 53(1_MeetingAbstracts):369